Original Article

JOURNAL OF COMPOSITE MATERIALS

Journal of Composite Materials
0(0) 1–18

DOI: 10.1177/0021998312470471
jcm.sagepub.com

SAGE

Influence of nitric acid treatment time on the mechanical and surface properties of high-strength carbon fibers

Tye A Langston and Richard D Granata

Abstract

High-strength carbon fibers were treated with nitric acid and periodically analyzed by several different methods to develop an understanding of overall property changes and how they relate to composite design. Fiber diameter, tensile strength, surface morphology, surface chemistry and surface energy were all evaluated as a function of treatment time and two distinct stages of change were identified; the first characterized by surface modification and the second by carbon material loss. Initially, the tensile strength, degree of surface oxidation and surface energy all increased. The surface oxidation consisted primarily of carbonyl and carboxylic acid types. Then in the second stage, both the tensile strength and surface oxidation reached stable levels and the fiber diameter began to rapidly decrease. The surface morphology and energy were the only properties that showed no obvious changes from one stage to the next. The surfaces were found to be smooth through all treatment times and the energy increased steadily throughout. It is believed that the variation of all of these properties is related to the fiber microstructure and how it varies through the cross-section of high-strength fibers. Specifically, high-strength carbon fibers are known to have better microstructural organization and alignment in the near-surface layer than within the interior.

Keywords

Carbon fiber, diameter, tensile strength, surface morphology, surface chemistry, oxidation, surface energy, nitric acid

Introduction

Carbon fibers exhibit exceptional properties, such as high stiffness and high specific strength, that make them excellent reinforcements for composite materials. However, the use of carbon fibers in composites is problematic because their native surface is relatively unreactive, leading to poor fiber/matrix interfacial bonding.[1–5] One method that is often implemented to improve the reactivity of carbon fibers is oxidation, which affects their surface morphology, tensile strength, surface functional chemistry and surface energy. Several different approaches are used to effect surface oxidation and can be categorized into either dry oxidation,[6,7] wet chemical oxidation[8–10] or plasma treatment.[11–14] In the following paragraphs, we consider the effects of various oxidative treatments on the different properties of carbon fibers.

Changes in surface morphology affect both fiber strength and fiber/matrix mechanical bonding and in turn, these changes lead to composite property changes. High-strength carbon fibers, being very brittle, are sensitive to material defects, both in their interior and on the surface. Different oxidative treatments affect the fiber surface morphology of carbon fibers in different ways and to different degrees. For example, using scanning electron microscopy (SEM) and atomic force microscopy (AFM), Nohara et al. evaluated the surfaces of high-strength (Toray T-300) carbon fibers after treatment with hydrochloric acid (HCl), nitric acid (HNO_3), as well as argon and oxygen plasmas. They found that while HCl had a smoothing effect, the other treatments roughened the surface by way of longitudinal striations.[10] Jain et al. also observed changes in high-strength carbon fiber (Toray T-300) roughness with HNO_3 treatment time as the fibers

Department of Ocean and Mechanical Engineering, Florida Atlantic University, Boca Raton, FL, USA

Corresponding author:
Tye A Langston, Department of Ocean and Mechanical Engineering, Florida Atlantic University, 777 Glades Road, Boca Raton, Florida, 33431, USA.
Email: tye.langston@navy.mil

first became smoother and then exhibited pitting with extended HNO_3 treatment times of up to 10 h.[15]

In addition to treatment type and exposure time, changes in the surface properties also depend on how the fiber is produced. High-modulus fibers, which are heat-treated at higher temperatures, generally have more organized microstructures than high-strength fibers and respond to surface treatments differently. Jain et al. showed differences in the response of the two fiber types to HNO_3 treatment in terms of changes in fiber tensile strength, surface roughness and composite material strength. Their high-modulus fibers (Toray X-340) exhibited little strength change, while their high-strength fibers (Toray T-300) exhibited a strengthening during initial treatment times that was followed by significant weakening with further HNO_3 treatment times. Overall, the high-strength fibers were much more responsive to the HNO_3 treatment and they attributed the initial observed strengthening to a smoothing of the fiber surface and the subsequent strength losses after prolonged treatment times to surface pitting.[15] Nohara et al. also observed fiber weakening with increased HNO_3 treatment time on high-strength (T-300) fibers but did not observe any strengthening during the initial stages of treatment.[10] Furthermore, not only does the microstructure vary between fiber types, it also varies within the fibers themselves. For example, Diefendorf and Tokarsky showed that for high-strength carbon fibers, the microstructure was better organized and aligned near the outer surface, or sheath, than it was in the interior regions.[16] This means that the material at the surface would be expected to respond differently to treatments than the inner material would if it was exposed.

The surface chemistry of a carbon fiber is also important from a composites viewpoint because it affects fiber interactions with the composite matrix resin. Chemical fiber/matrix bonding allows for the matrix to transfer loading to the stronger fibers, affecting both composite strength and toughness. Because fiber/matrix bonding is intimately dependent on the nature of the chemical bonding, it is imperative to know what functional groups are present on the surface of the fiber and in what concentrations. X-ray photoelectron spectroscopy (XPS) is commonly used to analyze carbon fiber surfaces as it provides an indication of the extent of oxidation. For example, Nohara et al. determined that wet chemical treatment with HNO_3 produced a higher level of oxidation compared to either hydrochloric acid, oxygen plasma or argon plasma treatments.[10] In theory, XPS can also be used to discriminate between different surface group types by using spectral deconvolution of the C(1s) region. However, the unambiguous identification of different functional groups on a fiber surface is often not possible because the C(1s) binding energy peaks of the different functional groups (e.g. hydroxyl, carbonyl and carboxylic acid groups) lie too close together for most XP spectrometers to fully resolve them. As a result, different oxides that exhibit similar binding energies are often grouped together when C(1 s) regions are deconvoluted. For example, Jang[17] and Chang[18] analyzed carbon fibers after oxygen plasma treatment and found that the overall level of surface oxygen increased significantly. The use of XPS peak-fitting techniques was used to divide the spectral envelope into three different groups (hydroxyl/quinine, carboxylic acid/ester and a CO_3/π–π^* shakeup peak), but they did not have sufficient resolution to quantify the individual oxides.

In the formation of a robust composite, fiber wettability also plays a vital role. If the matrix resin does not completely wet the fibers, the composite suffers from internal voids that reduce the amount of fiber/matrix interfacial contact and this in turn creates stress concentrations. Estimates of fiber wettability can be ascertained by using individual fiber contact angles to determine surface energies in accordance with the methods described by Kaelble et al.[19] In general, it is believed that increases in surface energy lead to improved fiber wettability. Surface energy, which is composed of polar and dispersive components, has been observed to change as a result of different fiber treatments. For example, after oxygen plasma treatment, Jang[17] and Chang[18] found that the polar surface energy generally increased while the dispersive energy decreased. The total surface energy, which is a linear combination of the polar and dispersive components, increased significantly, although they did observe a slight reduction after prolonged plasma treatment, a phenomenon they attributed to fiber pitting. Based on the overall surface energy increase, they deduced that the oxygen plasma treatment made the fibers more wettable and that this increased single-fiber wettability would translate into improved fiber/matrix wetting in composites. A similar analysis is applied in the present investigation for fibers treated with HNO_3, where the polar and dispersive contributions to the surface energy are calculated by measuring contact angles in different liquids.

Amongst these various treatment strategies, immersion in heated HNO_3 is known to be a very effective wet chemical oxidation method,[8–10] but its exact effects on fiber properties have not been fully elucidated, including the effect of treatment time. Before a modified fiber type is incorporated into a composite, it is important that all of the treatment effects are understood and quantified. Without developing this information, it is difficult to understand the underlying causes of composite property changes or develop improved fiber

modification strategies. To address this issue, the focus of this study has been to investigate the effects of HNO_3 treatment time on the mechanical and surface properties of carbon fibers.

Materials

Two types of carbon fibers were analyzed. The first was Hexcel Company's unsized AS4 and the second was Toray Industries' T700, which came pre-coated with type FOE sizing. The FOE designator describes the sizing type, surface treatment and sizing amount. Specifically, an oxidizing surface treatment was applied, this sizing is compatible with vinyl ester and epoxy, and the amount applied is 0.7%. Both fiber types qualify as high-strength (Type II) and exhibit similar physical properties (tensile strength, tensile modulus, strain at break and density). By comparing similar fibers from two different manufacturers, it helps to demonstrate that the behaviors observed are not specific to one manufacturer's fiber. The sized fiber (T700) represents what can be commonly attained from manufacturers, while unsized fibers are much more difficult to find. By comparing as-received sized fibers to HNO_3-treated fibers, one can ascertain whether advantages are gained over what is typically acquired from manufacturers. Both fiber types were subjected to oxidizing surface treatments from the manufacturer, but due to diameter reductions resulting from the treatments applied herein, the manufacturer treatments were not believed to have an effect on the subsequent treatments applied in this study. Concentrated HNO_3 (70%, NF grade) was used as the oxidant. To quantify surface functional group concentrations, five chemicals were used in the three chemical derivatization reactions: trifluoroacetic anhydride (TFAA), trifluoroethyl hydrazine (TFH), trifluoroethanol (TFE), di-tert-butylcarbodiimide (DTBC) and pyridine.

Experimental methods

Fiber surface oxidation

Acid treatment was accomplished by wrapping fiber tows around glass frames and securing them on the ends with PTFE tape. To prepare the fibers for oxidation, they were first subjected to a 2-h distilled water wash at room temperature, followed by a 2-h drying period at 120°C. Fibers were then oxidized to differing degrees by immersing them in refluxing HNO_3 at 120°C. The degree of oxidation was controlled by varying the length of acid exposure time, which spanned from 0 to 160 min. After acid exposure, the fibers were again washed repetitively in refreshed baths of distilled water, until the pH of the wash water had stabilized between successive water changes and was within 0.1 of that of the pure distilled water. Following the final wash, the fibers were subjected to another 2-h drying period at 120°C and then stored under vacuum with a silica gel desiccant until the treated fibers were characterized.

Fiber surface morphology and diameter

Fiber surface morphology and diameter were analyzed by viewing and measuring fibers in a Quanta 200 (FEI Company) SEM at 5000 times magnification. Images were first acquired by SEM and measured with Scandium® SEM image analysis software. Both fiber types were analyzed in the same way and at least 10 samples were used to determine an average fiber diameter for each HNO_3 treatment time.

Fiber tensile strength

Fiber tensile strength was determined by testing single filaments in accordance with ASTM D 3379-75 protocols to determine the load at break. Average fiber diameters for each treatment time were then measured by SEM and the strengths were calculated by dividing the loads by the average diameters. Both fiber types were evaluated in the same way and at least 20 fibers were tested for each HNO_3 treatment time.

To test the tensile strength of an individual fiber, it was first glued to a fixture, as shown in Figure 1. The fixture was cut from paper and cyanoacrylate (super) glue was used to attach the fiber. After allowing the glue to dry, the fixture was placed into the grips of a tensile-testing machine (aligning the grip ends with the cross-hatched markings to assure alignment) and the sides of the paper fixture were cut away so that only the fiber was stressed during testing. A MTS 2 N load cell, mounted on a MTS Insight 1 kN test stand, was used at a crosshead speed of 0.5 mm/min, which resulted in a test time of approximately 1 min (as recommended by ASTM D 3379-75). ASTM D 3379-75 allows for gage lengths from 20 to 30 mm to be tested. The 20 mm length was chosen because calibration tests performed at this length provided the closest agreement between untreated fiber strengths and the

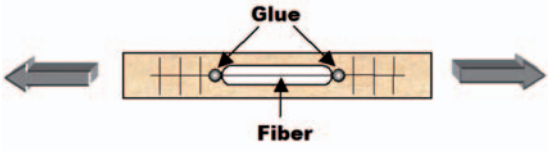

Figure 1. Single-fiber tensile test fixture.

manufacturers' reported values (0.2 and 12 percent variation for the AS4 and T700 fiber types, respectively).

Fiber surface chemistry

Fiber surface chemistry was evaluated by a combination of XPS and chemical derivatization. XPS was used to determine the overall amount of surface oxygen, nitrogen and carbon on the fibers and chemical derivatization was applied to quantify specific functional groups (hydroxyl, carbonyl and carboxylic acid). Both types of untreated fiber were analyzed, as well as HNO_3-treated AS4 (unsized) fibers after 5, 20, 40, 80 and 160 min of treatment.

XPS analysis was carried out in a PHI 5400 ($P_{base} \approx 1 \times 10^{-8}$ Torr). All XP spectra were acquired with a non-monochromatic Mg K_α (1253.6 eV) X-ray source operating at 15 kV and 300 W. Elemental scans were acquired using a pass energy of 178.95 eV and a resolution of 0.250 eV/step. Binding energies were referenced to the C–C/CH_2 component of the C(1 s) region centered at 284.5 eV.[20]

Vapor-phase chemical derivatization was conducted in accordance with Langley et al.[21] TFAA, TFH and TFE were used in separate reactions as derivatizing reagents to determine the concentration of surface hydroxyl, carbonyl or carboxylate groups, as described in Figure 2, in conjunction with XPS compositional analysis. In each derivatizing reaction, fluorine-containing reagents were chosen because of the high XPS cross-section of fluorine atoms and the fact that fluorine in not an indigenous element present on carbon fibers.

Fiber surface energy

Fiber surface energy was determined by the micro Wilhelmy plate technique, as described by Kaelble et al., which involves inserting and extracting single fibers through test liquids and measuring the contact forces.[19] With these forces, contact angles were calculated using the equation described by Neumann and Tanner[22] and Mozzo and Chabord[23]:

$$\theta = \arccos\left(\frac{Mg}{C\gamma_{LV}}\right) \quad (1)$$

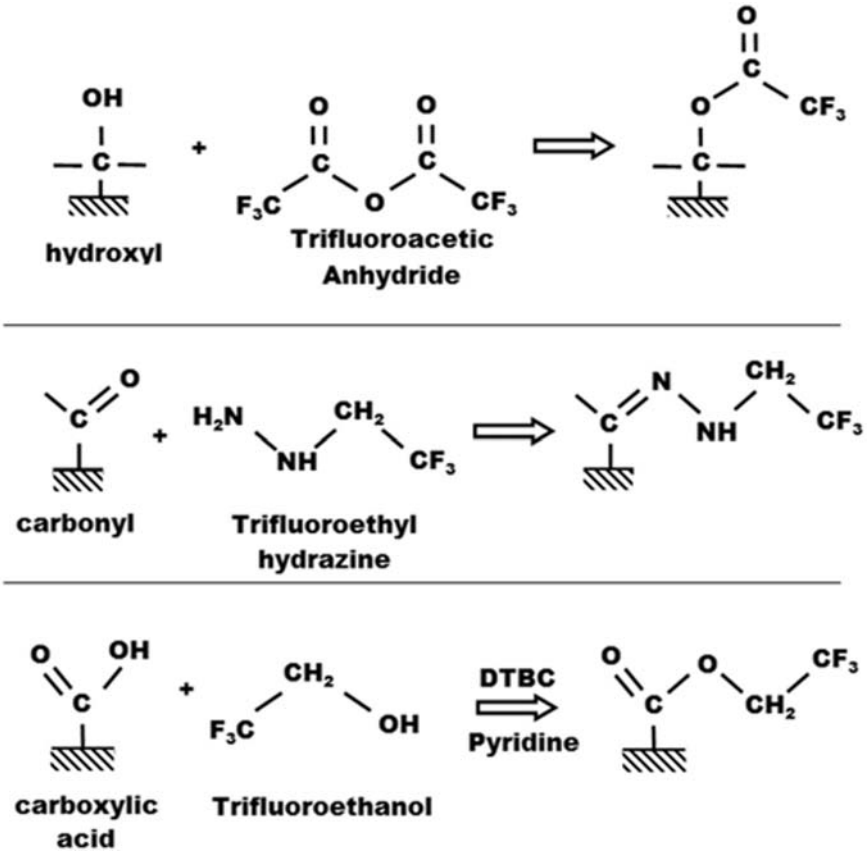

Figure 2. Target surface oxides, derivatizing agents and surface products of the three derivatization reactions.

where θ is the advancing contact angle, M is the contact force, C is the fiber circumference, γ_{LV} is the liquid-vapor surface tension and $g = 980.6\,\text{dyn/gm}$. The micro Wilhelmy plate method is depicted in Figure 3.

Once θ was determined, the Young-Dupre equation was then applied to obtain the reversible work of adhesion (W_a):[19]

$$W_a = \gamma_{LV}(1 + \cos\theta) \tag{2}$$

Using W_a and the known polar (Kesesom-p) and dispersive (London-d) properties of the test liquids, a plot was generated whose slope and intercept corresponded to the polar and dispersive energy components of the fiber surface.[19] For such analysis, at least two different liquids that differ significantly in terms of their polarity are required to assure that measurements reflect the different contributions to the surface energy. In light of this requirement, water (polar) and diiodomethane (non-polar) were chosen as test liquids in the present investigation.

The fiber/liquid contact force was measured using a CAHN DCA-322 Dynamic Contact Angle Analyzer with WinDCA32 software. Five to ten separate fibers were analyzed for each fiber surface condition (sized, unsized and treated) and each fluid used (water and diiodomethane). The CAHN DCA-322 electrobalance has a sensitivity of $\pm 0.1\,\mu\text{g}$. The fiber circumference was determined by measuring the diameter of each fiber before analysis, using a Mitutoyo LSM-6200 Laser Scan Micrometer. Two to three diameter measurements were taken along the immersion length of each fiber and averaged. Both types of untreated fiber were analyzed, as well as HNO_3-treated AS4 (unsized) fiber after 40, 80, 120 and 160 min HNO_3 treatment times.

Results

Fiber surface morphology and diameter

Irrespective of the HNO_3 treatment time, SEM analysis revealed that major fiber surface defects were virtually nonexistent. Intensive searches eventually yielded surface flaws in a few cases, but they were rare and random SEM spot-checks showed fibers that were almost always completely smooth, except for gently rolling grooves and striations that could be seen both before and after HNO_3 treatment. Figure 4 provides an example of a flaw that was found after extensive searching while Figure 5 shows the typical fiber surfaces. The few flaws that were observed may have resulted from physical damage or fiber material irregularities that were predisposed to acid attack. Fiber surface roughness can affect both the fiber strength and composite fiber/matrix bonding; increased roughness weakens fibers through stress concentrations, but it also allows for better mechanical bonding to the matrix. Based on the lack of physical surface changes as viewed through SEM analysis, neither fiber weakening nor improved composite fiber/matrix mechanical bonding would be expected.

Some carbon fiber treatment methods are known to cause significant surface degradation that is easily viewable by SEM,[10,17,18] but that does not appear to be the case in the present study. However, while the SEM images revealed few observable changes in fiber surface morphology, they did reveal significant reductions in fiber diameter, especially at longer HNO_3 treatment times, indicating that fiber volume was being removed. Thus, Figure 6 shows a plot of the average AS4 (unsized) and T700 (sized) fiber diameters as a function of HNO_3 treatment time. A significant diameter reduction can be seen in both fiber types with HNO_3 treatment times in

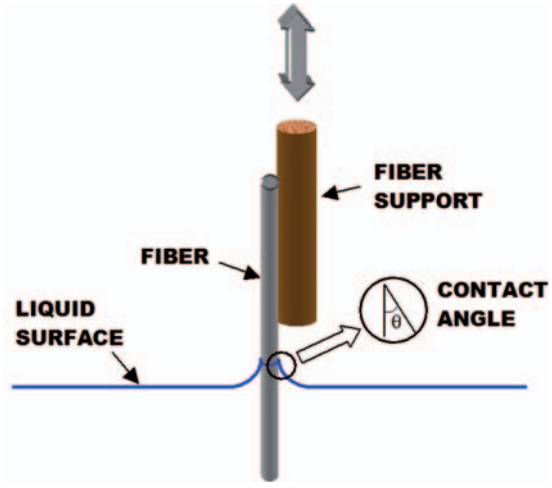

Figure 3. Micro Wilhelmy plate method of measuring contact angle.

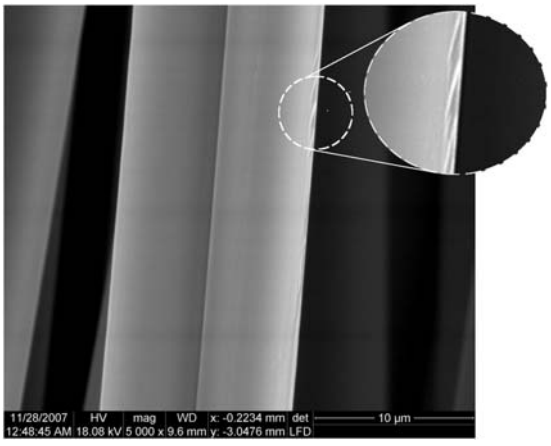

Figure 4. Example of a fiber flaw identified after extensive searching (T700 (sized) – 160 min HNO_3 treatment).

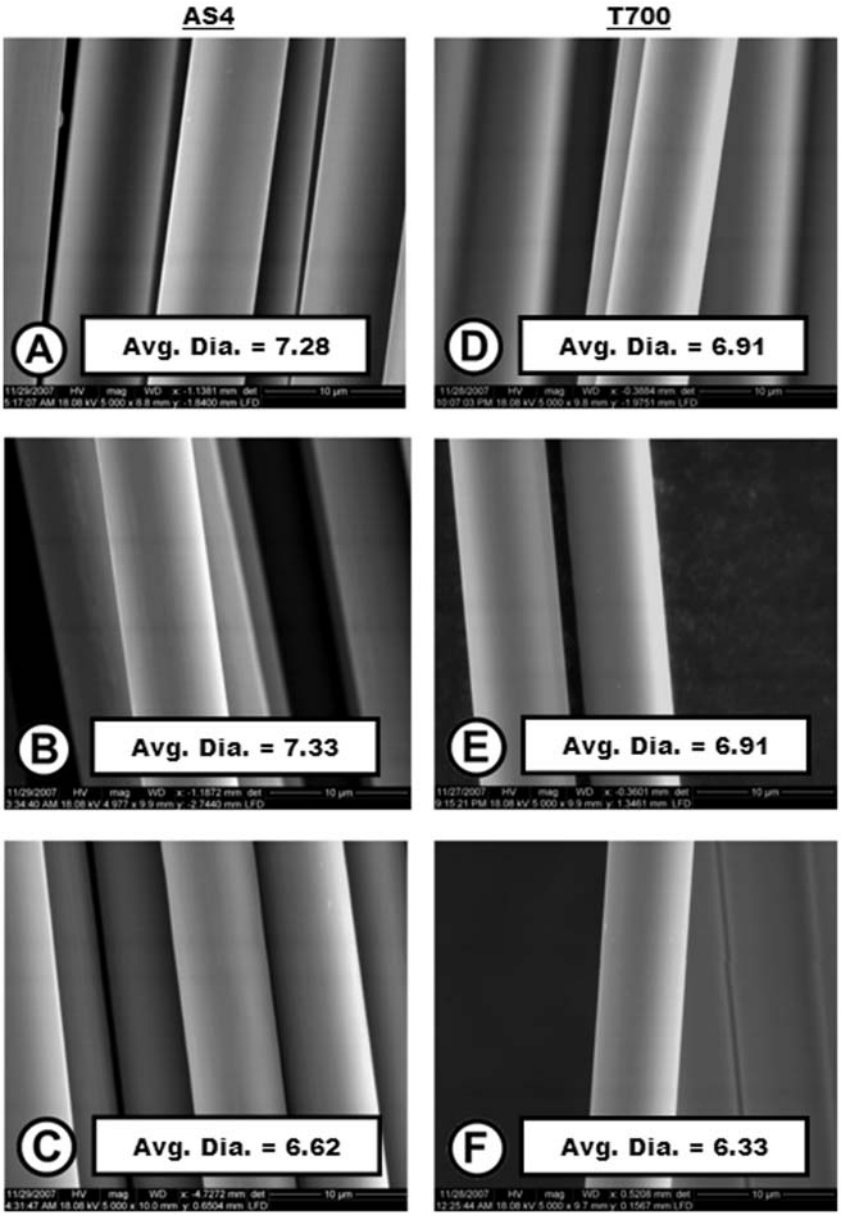

Figure 5. Carbon fibers at different stages of HNO_3 treatment: (A) AS4 (unsized) fiber, untreated, (B) AS4 (unsized) fiber, 40 min treatment, (C) AS4 (unsized) fiber, 160-min treatment, (D) T700 (sized) fiber, untreated, (E) T700 (sized) fiber, 40 min treatment, (F) T700 (sized) fiber, 160-min treatment.

excess of approximately 40 min, with the largest changes observed after 160 min. At this longest treatment time, the average T700 (sized) and AS4 (unsized) diameters decreased by 8.4% and 9.1%, respectively (corresponding to a fiber volume loss of 16.1% and 17.4%).

Thus, HNO_3 treatments appear to have a much more significant effect on high-strength fiber diameter than they do on the creation of surface flaws. Because measureable changes in fiber diameter were observed during acid treatment, it also becomes a necessary variable to consider when evaluating the strength of these fibers treated with HNO_3.

Fiber tensile strength

Although single fiber tensile testing provides an indication of fiber *load* at failure, diameter changes during HNO_3 treatment must also be considered in order to correctly evaluate fiber *strength*. Our results show that with respect to HNO_3 treated fibers, it is not appropriate to simply use the average diameter of the untreated fibers, as is often done. Plotted as a function of HNO_3 treatment time, Figure 7(a) shows the average fiber *load* at failure, while Figure 7(b) takes the average fiber diameter into account to determine average fiber *strength*.

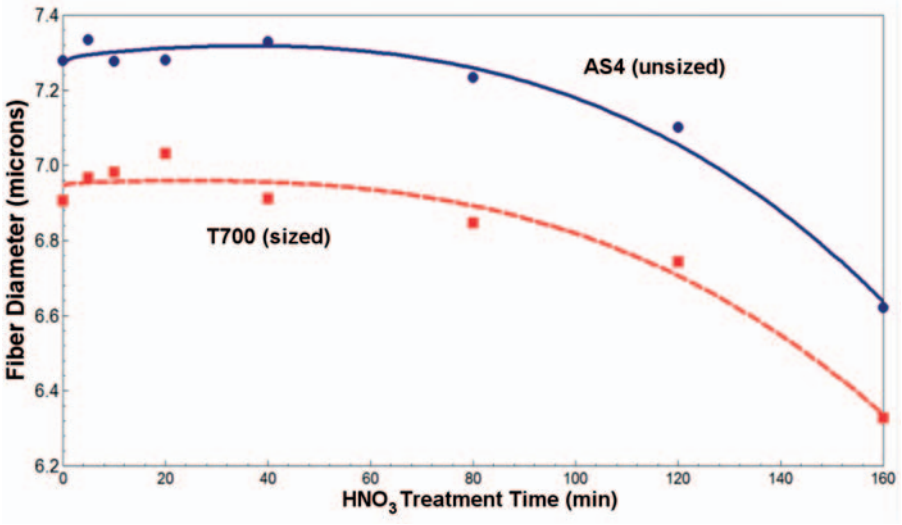

Figure 6. Fiber diameter as a function of HNO_3 treatment time.

Based on failure *load* data alone (Figure 7(a)), the conclusion would be that the fibers reach their peak *strength* around 40 min HNO_3 treatment time, followed by a decline in fiber strength for longer HNO_3 treatment times. And if a constant fiber diameter was used to calculate strength, the strength curve would mirror this load curve trend. However, when fiber diameter changes are considered as well (Figure 7(b)), it becomes clear that the fibers attain an improved strength after HNO_3 treatment and that this enhanced strength remains approximately constant for treatment times in excess of 20 min. Thus, after an initial strengthening in the early stages of treatment, fibers do not actually lose any *strength*, they just lose cross-sectional *area* with extended treatment times. The long-term increase in strength was found to be approximately 20% and 15% for the T700 (sized) and AS4 (unsized) fibers, respectively. However, it should be noted that while both fiber types generally showed an improvement in strength after most HNO_3 treatment times, they also exhibited a short-lived decline in strength for the shortest (5 min) treatment time.

Fiber surface chemistry

Prior to HNO_3 treatment, the surface chemistry of both the untreated AS4 (unsized) and T700 (sized) fiber types was analyzed. After HNO_3 treatment, only the surface chemistry of the AS4 (unsized) fibers was studied. The primary reason for this decision was that the sizing is not expected to significantly affect the fibers after HNO_3 treatment because it is a thin surface layer that is quickly removed by the acid. This is consistent with the fact that the fiber strengths and diameters for both the treated and untreated fibers show similar variations with HNO_3 treatment (see Figure 7(b)). Furthermore, the sizing material composition is proprietary and introduces an unknown variable, particularly with respect to the detailed chemical surface composition.

AS4 (unsized) fiber surface chemistry. The surface composition of the AS4 (unsized) fibers was determined with XPS before and after HNO_3 treatment by analyzing the photoelectron peaks and integrating the peak areas. All fibers contained carbon, oxygen and nitrogen. The largest change in chemical composition upon HNO_3 treatment was an increase in the level of total oxygen concentration, as shown in Figure 8 by the growth of the O(1 s) peak.

Although the inclusion of nitrates onto the surface is plausible when HNO_3 is used as the oxidizing agent, the XPS analysis shows that there is little change in the overall nitrogen content of the fibers, even with extended HNO_3 treatment time (Table 1). Thus, the dominant chemical effect of HNO_3 treatment on surface composition involves the introduction of polar oxygen-containing functional groups onto the fiber surface.

By analyzing the line shape of the C(1 s) spectral envelopes shown in Figure 8, it is possible to derive a rough sense of the functional groups present on the sample. For example, the 40 and 160 min HNO_3-treated fibers show a spectral feature centered around 288.5 eV, indicative of photoelectrons from carbon atoms at the surface in highly oxidized environments (e.g. carboxyl or ester groups). The line shape and peak position in the O(1 s) region also evolves with HNO_3 treatment time, shifting to lower binding energies for longer HNO_3 treatment times, representative of the formation of more electron-rich oxygen species, such as COOH.

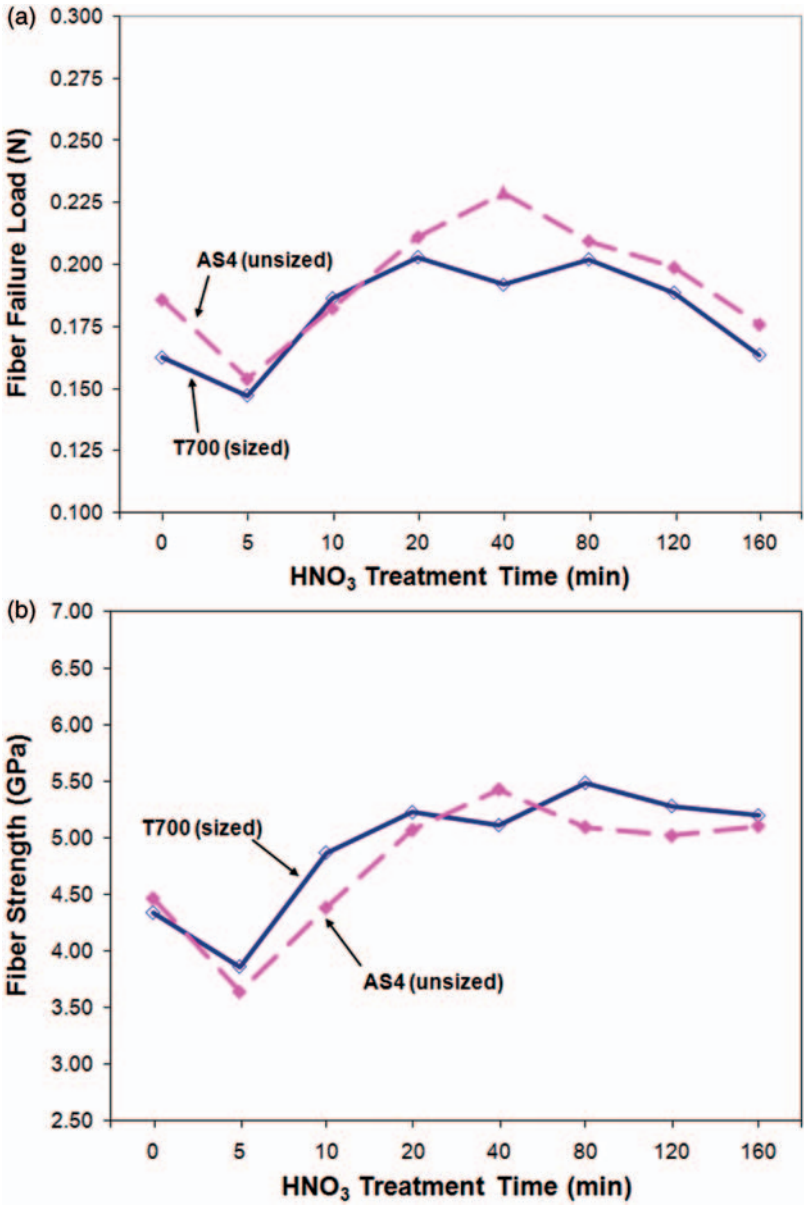

Figure 7. (a) Average fiber load at failure as a function of HNO_3 treatment time. (b) Average fiber strength as a function of HNO_3 treatment time.

However, by using chemical derivatization, more detailed and unambiguous information about the nature and concentration of oxygen-containing functional groups can be ascertained. Figure 9 shows the results of the chemical derivatization experiments performed in conjunction with XPS analysis that allowed quantification of the relative concentrations of hydroxyl, carbonyl and carboxylic groups on native and HNO_3-treated carbon fiber surfaces (see Figure 2 for derivatization reactions).

The untreated, AS4 (unsized) fiber surface oxidation consisted almost entirely of hydroxyl, carbonyl and carboxylic groups, with minimal ''residual'' oxides that cannot be quantified with the chemical derivatization strategies employed in this investigation. The ''residual'' category has several possibilities, including pyrones, lactones, anhydrides, esters and ethers,[24–30] as well as oxides that are too closely located on the surface to permit 100% derivatization (sterically hindered). Analysis of Figure 9 reveals that HNO_3 treatment caused a gradual increase in both carboxylic acid (COOH) and carbonyl (C = O) groups for HNO_3 treatment times less than 40 min. For more prolonged treatment times, their concentrations remained roughly constant. Although the carboxylic acid group concentration doubled compared to the value obtained for the

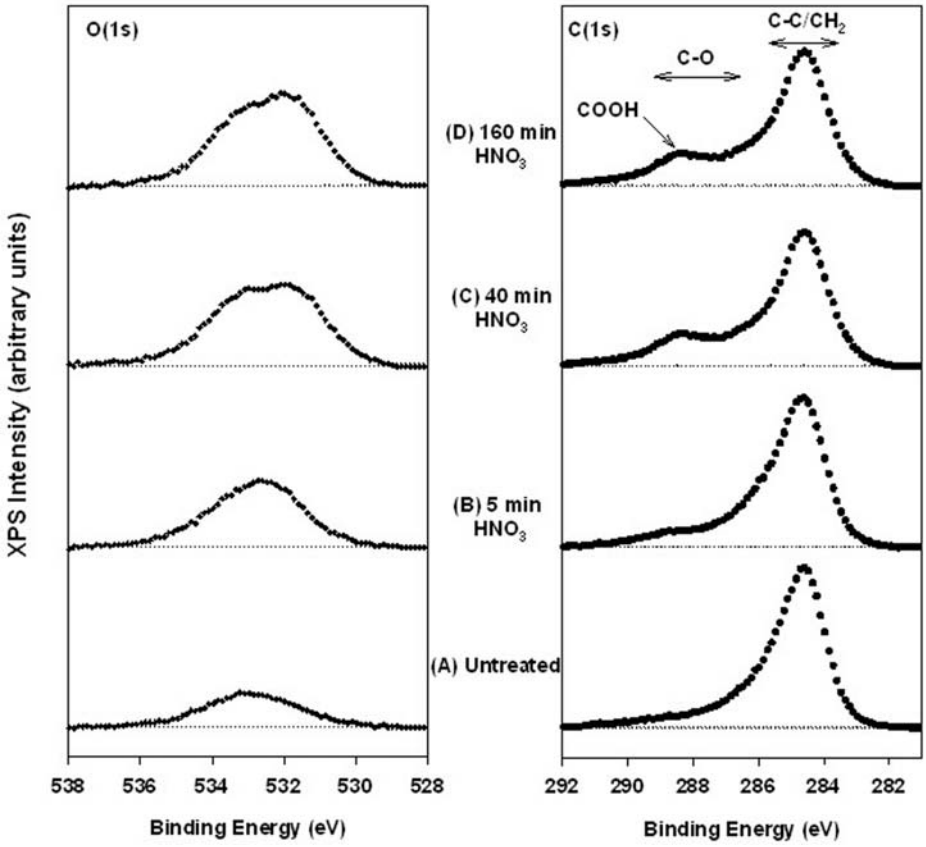

Figure 8. XP spectra of the O (1 s) and C (1 s) regions of the (A) AS4 (unsized) untreated fiber, (B) AS4 (unsized) 5-min HNO_3-treated fiber, (C) AS4 (unsized) 40-min HNO_3-treated fiber and (D) AS4 (unsized) 160-min HNO_3-treated fiber.

Table 1. Surface concentration of nitrogen atoms as determined by X-ray photoelectron spectroscopy (XPS) before and after HNO_3 treatment for AS4 (unsized) fibers.

	Nitrogen surface concentration			
	Untreated	5 min HNO_3	20 min HNO_3	80 min HNO_3
Concentration (%)	2.6	2.0	2.3	1.9

untreated fiber and the carbonyl group concentration tripled, the hydroxyl group concentration actually declined. This suggests that in addition to grafting new oxygen-containing functional groups, HNO_3 also converts existing oxides on the untreated carbon fiber surface into more highly oxidized functional groups. Figure 9 also shows that the ''residual'' oxide group concentration initially increased but then decreased for HNO_3 treatment times in excess of 40 min.

T700 (sized) fiber surface chemistry. The untreated T700 (sized) fibers differ significantly from the AS4 (unsized) fibers in that they have a proprietary coating intended to aid in the processing, handling and fiber/matrix bonding of the fibers. Although the exact composition of the coating is unknown, it is believed to be polymeric. As expected, the surface chemistry analysis of the untreated T700 (sized) fibers yielded very different results than that of the AS4 (unsized) fibers. Figure 10 compares their surface concentrations, determined through XPS and chemical derivatization.

With respect to the surface concentration of hydroxyl, carbonyl and carboxylic acid groups, the untreated T700 (sized) fibers are similar to the untreated AS4 (unsized) fibers but differ significantly in the overall level of surface oxidation. Overall, the untreated T700 (sized) fibers have a much higher level of oxidation and the majority of their oxides fall into the ''residual'' category, which cannot be characterized by our chemical derivatization methods (i.e., they are not hydroxyl, carbonyl or carboxyl groups). Analysis of the C(1 s) spectral envelope for the sized fibers (data not shown) suggests that ethers or esters are an important component of these ''residual'' oxides. Like the AS4 (unsized) fibers, the T700 (sized) fibers also had a low surface concentration of nitrogen atoms (1.4%).

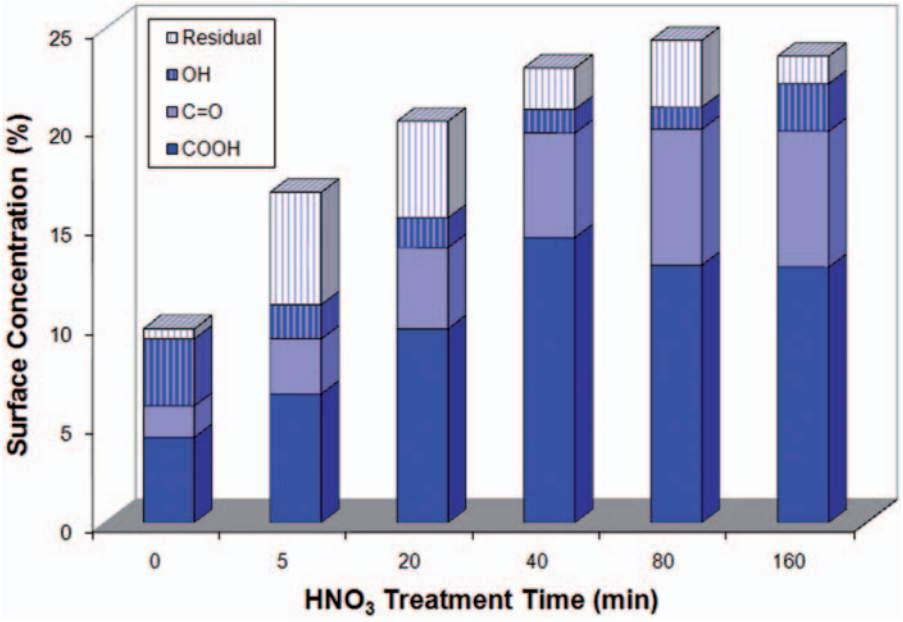

Figure 9. Surface oxygen functional group distribution of native and HNO_3-treated AS4 (unsized) fibers as determined by chemical derivatization in conjunction with X-ray photoelectron spectroscopy (XPS) analysis.

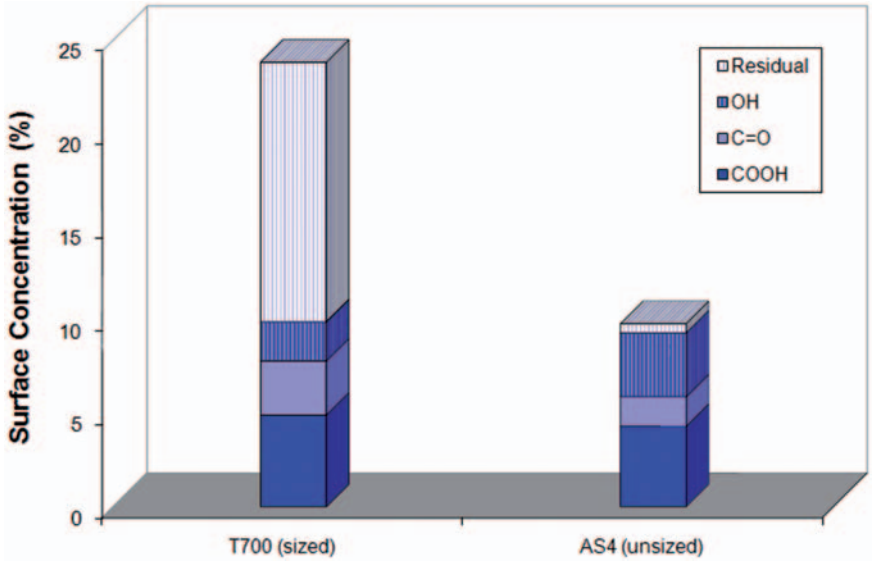

Figure 10. Distribution of surface oxygen functional groups of untreated T700 (sized) and AS4 (unsized) fibers as determined by chemical derivatization, used in conjunction with X-ray photoelectron spectroscopy (XPS).

Fiber surface energy

Fiber surface energy was evaluated for both the untreated T700 (sized) and AS4 (unsized) fiber types. After HNO_3 treatment, only the surface energy of the AS4 (unsized) fibers was evaluated for the same reasons mentioned above in the surface chemistry results section. Namely, the sizing was not expected to significantly affect the results because it should be rapidly removed during HNO_3 treatment and the proprietary sizing material introduces an unknown variable. This assertion is also supported by the similar mechanical properties and similar responses to acid treatment (e.g., surface roughness, strength change and diameter change) observed for both fiber types.

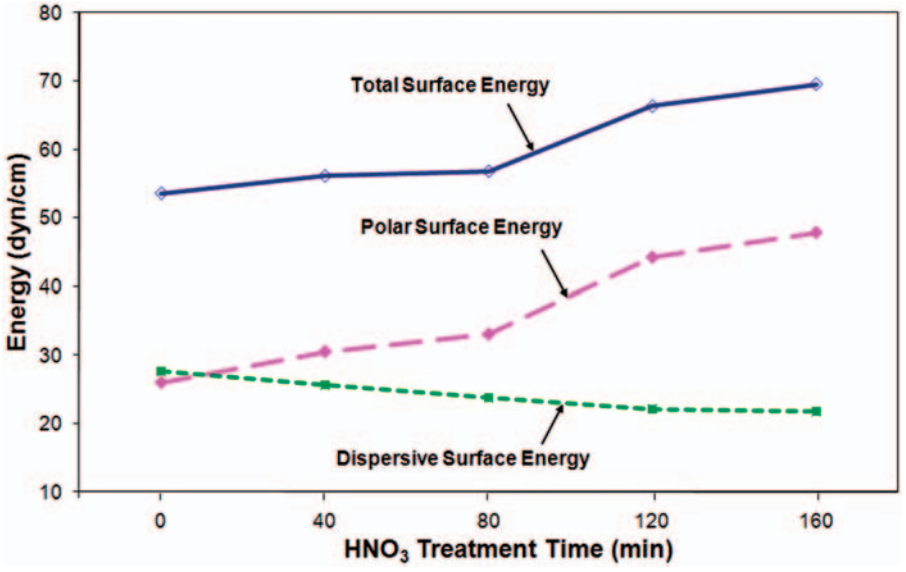

Figure 11. AS4 (unsized) fiber surface energy (polar, dispersive and total) as a function of HNO_3 treatment time.

AS4 (unsized) fiber surface energy. HNO_3 treatment of the AS4 (unsized) carbon fibers alters their surface energy significantly. Polar, dispersive and total energies were all affected as Figure 11 indicates.

From Figure 11, it can be seen that the polar and dispersive energies were approximately equal on the untreated AS4 (unsized) fibers (HNO_3 treatment time, $t = 0$). The polar component of fiber surface energy, γ_{SV}^{P}, continually increased with HNO_3 treatment time, from 26.0 dyn/cm up to a maximum of 47.8 dyn/cm, and the dispersive energy, γ_{SV}^{d}, showed the opposite trend, decreasing from 27.6 dyn/cm to 21.7 dyn/cm. Even after the maximum treatment length of 160 min, the surface energy had not stabilized. Despite the continued changes, a longer HNO_3 treatment time was not pursued because this would have lead to substantial losses in fiber diameter and carbon material. Simply put, it is not believed to be practical from a composites standpoint to purchase fibers and then remove a large amount of their bulk before use, even if an increase in surface energy can be attained.

The total fiber surface energy is the summation of the polar and dispersive energies and in this case, it is dominated by the polar component on HNO_3-treated fibers. As a result of changes in the polar energy, the total fiber surface energy increased monotonically with HNO_3 treatment time due at least in part to the addition of the highly polar oxygen-containing functional groups. It increased from 53.6 dyn/cm in the untreated condition to 69.6 dyn/cm after 160 min of HNO_3 treatment. According to existing wettability theories, the increase in solid-vapor surface energy indicates that these carbon fibers are likely to be more easily wetted by matrix resins after HNO_3 treatment.

Untreated T700 (sized) fiber surface energy. The differences in the surface energy of the untreated sized and unsized carbon fibers are shown in Figure 12. The untreated T700 (sized) fibers had a slightly higher dispersive energy and lower polar energy than the AS4 (unsized) fibers. The T700 (sized) fiber's total surface energy was slightly less than that of the AS4 (unsized) fiber, but the difference was minimal. Therefore, we would predict that both the untreated sized and unsized fibers would exhibit similar wettabilities.

Discussion

HNO_3 treatment affects both the physical and chemical characteristics of carbon fibers, which in turn will affect the properties of composites made with these fibers. Consequently, it is imperative to first understand how treatment time affects the fiber characteristics, such as size, strength, surface morphology, surface chemistry and surface energy, so that resultant composite property changes (i.e., fiber/matrix ratio, strength, fiber/matrix mechanical and chemical adhesion, interphase properties and void content) may also be understood.

Our results indicate that the length of treatment plays a big role in what properties should be expected from HNO_3-treated high-strength carbon fibers. Specifically, it was observed that fiber changes fall into two regimes; the first characterized by surface modifications and the second associated with carbon material loss. During the first stage, surface changes are directly evident through increasing concentrations of oxidizing functional groups, as well as rising polar surface energy and falling dispersive energy. Fiber strength also increases during this stage, which may

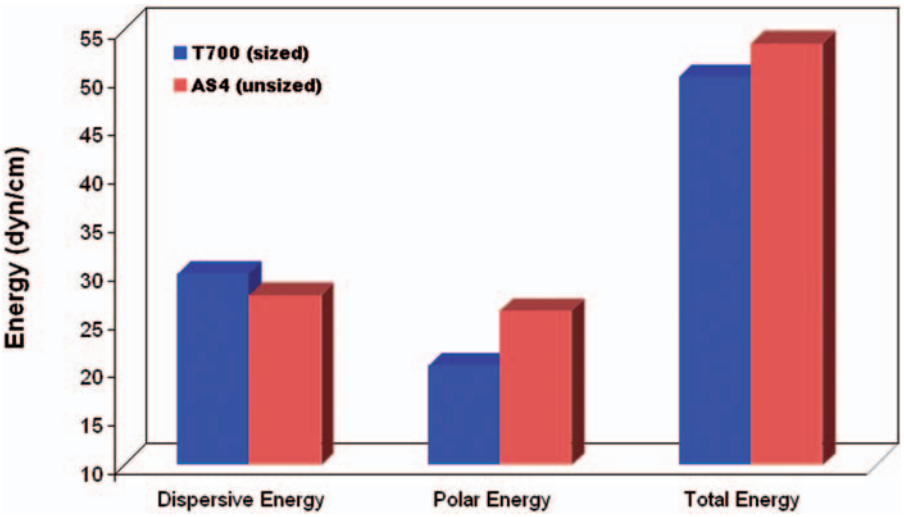

Figure 12. Untreated AS4 (unsized) and T700 (sized) fiber surface energy (polar, dispersive and total).

too be attributed to changes at the fiber surface. Then, during the second stage of treatment, both the surface chemistry and fiber strength stabilize, and the overall fiber diameter begins to decline as bulk carbon material is lost. The fiber surface energy, however, shows very little change from one stage to the next, continuing on its path of rising polar energy and falling dispersive energy.

(i) Influence of HNO_3 treatment on fiber strength

Fiber strength was found to increase with HNO_3 treatment time up until about 20 min, at which time it stabilized to a constant level. The observed fiber strengthening is likely due to a couple different changes that result from the HNO_3 treatment: (a) removal of the outer fiber layer, or sheath, which has different graphitic structure than the core and (b) mitigation of small-scale flaws.

One of the most obvious changes we observed with HNO_3 treatment was reduced fiber diameters at extended treatments times. In the context of composite design, this diameter reduction may not be as significant a problem as it first appears. In fact, it is actually beneficial. Speaking purely in geometric terms, while smaller fibers cannot individually support as large of loads as bigger fibers can, they require less space and allow for additional fibers to be packed into a given volume. Indeed, a composite's maximum fiber volume fraction is independent of fiber diameter.[31] And when looking beyond fiber geometry alone, it becomes apparent that when you factor these diameter changes into fiber strength calculations, the fibers actually become *stronger* as a result of HNO_3 treatment. These diameter reductions are not just a benign byproduct of HNO_3 treatment, instead, they likely play a key role in the mechanism of fiber strengthening. The graphitic structure of carbon fibers is not uniform. In fact, the outer layer, known as the sheath, is significantly different from the core, according to Diefendorf and Tokarsky, who analyzed various carbon fiber types using X-ray diffraction, electron diffraction, bright field microscopy, dark field microscopy, replication electron microscopy, SEM, optical polarized light microscopy and reverse radio frequency sputtering. They found that the basic structure of carbon fibers consists of rippled ribbons that make up roughly parallel layers of basal planes along the fiber axis. When considering PAN-based fibers with similar moduli as those investigated herein, they reported that the graphitic basal planes are much better aligned in the near-surface sheath than in the fiber interior. The graphitic ribbons of the core exhibit much more irregularity. They can be folded, layered or radial in structure.[16] Naturally, one would expect the outer, more aligned, layer to exhibit different physical properties and acid resistance than the core.

The longer a fiber is heat-treated, the more organized and aligned the graphitic planes generally become[15,16] and it is believed that when a fiber is allowed to cool with different graphitic organizations in its core and sheath, it leads to a couple different types of stress problems. First, the non-homogeneity in material structure across the section leads to residual stresses within the fiber.[16] Furthermore, when such a fiber is subjected to external force, a non-uniform stress profile arises between the core and surface.[16,32] Diefendor and Tokarsky indicated that this variation in axial preferred orientation will cause the outside sheath to disproportionately carry more of the fiber load.[16] Both the residual stresses and non-uniform stress profile may contribute to fiber cracking and the associated deterioration of tensile strength. Removal of this

different outer layer by HNO_3 exposure leads to a fiber with more uniform microstructure across its section as the less-organized graphitic structure of the core gradually emerges at the surface. This, in turn, results in lower residual stresses, more consistent loading across the fiber and, ultimately, higher strength.

The variation in sheath material properties may also help to explain the slower reduction in diameter observed in the early stage of HNO_3 exposure. The outer, more highly organized graphitic layer is likely more resistant to acid attack than the less-organized core. Differences in the acid resistance between more and less-organized graphitic structures may be better understood through general comparisons between high-strength and high-modulus carbon fibers. Overall, high-modulus fibers are heat-treated longer and consequently have more organized graphitic structures than high-strength fibers do.[15,16] With increasing moduli, the graphitic ribbons become thicker, straighter and better aligned along the fiber axis. One example of these differences comes from Jain et al. who compared the weight loss of both high-strength and high-modulus carbon fibers after concentrated HNO_3 exposure. They found that high modulus fibers are generally more resistant to acid attack. After 15 min of exposure, their high-strength fibers lost 9% of their weight, while their high-modulus fibers only lost 4.8%. Furthermore, their high-modulus fibers ceased to lose weight after 15 min of exposure, while the high-strength fibers continued to break down. Their high-strength fibers lost 18% of their weight by 1 h and completely disintegrated within 5 h of exposure.[15] This illustrates that HNO_3 resistance is highly dependent on the degree of microstructural organization of the fibers. And as Diefendorf and Tokarsky showed, the degree of organization varies between the sheath and the core in high-strength carbon fibers.[16]

We have discussed the differences in material properties in the outer fiber layer and how they may lead to fiber weakening through residual stresses and non-uniform stress distributions under load. Additionally, just because we did not directly observe any surface flaws on the untreated fibers with SEM, the likely impact of small defects on as-received fiber surfaces should not be completely discounted. Just because no flaws were observed does not mean that flaws were not present. It just means that no *major* flaws were found that could be identified with the limited resolution available with SEM analysis. In fact, using AFM, which is capable of greater resolution than SEM, Nohara et al. showed that as-received carbon fibers can indeed exhibit small-scale surface roughness in the form of grooves and striations. However, this also depends on the nature of the fibers and some fiber types will be rougher than others. Diefendorf and Tokarsky, for example, showed that lower modulus fibers have naturally smoother surfaces than high-modulus fibers do.

Based on the principal properties of high-strength carbon fibers and the Griffith theory of fracture mechanics,[33] we do know that their strength is highly dependent on flaws, and therefore one of the best indicators of flaw existence may be the fiber strength itself. And due to processing and handling during manufacture and use, fibers would be expected to sustain some sort of physical surface damage. Being a material of very high strength and stiffness, carbon fibers naturally have low fracture toughness, and the literature yields several indications of their flaw sensitivity. First, the strength of carbon fibers falls way short of theoretically predicted values that suggest they should be able to withstand up to 180 GPa. In actuality, the practical strength of most fibers falls within the range of 3 to 20 GPa.[32] In addition to physical surface damage, flaw types may include, for example, inorganic inclusions, organic inclusions, irregular voids from rapid coagulation and cylindrical voids precipitated from dissolved gases.[32]

Another convincing indication of the flaw sensitivity of carbon fibers comes from their strength dependence on gage length. Basically, longer fibers are weaker because there is a higher probability that they contain significant defects.[32,34] Relying on this premise, Pickering and Murray statistically evaluated carbon fiber strength/gage length relationships by applying the two-parameter Weibull approach to weak-link scaling.[34] Weak-link scaling is a statistical strength prediction approach that is only applicable to brittle, flaw-sensitive materials. It contends that if a material is sufficiently flaw-sensitive, it can only be as strong as its weakest link (i.e., worst flaw). They found that the shorter specimens were, on average, stronger than the longer ones, due to the lower probability of significant flaws. Furthermore, we also directly tested this theory and found this gage length/strength relationship to be true for the untreated T700 (sized) fiber type. It exhibited strength increases of 13% and 23% when the test gage length was shortened from 30 mm to 25 mm and then from 25 mm to 20 mm, respectively. This test indicates both that flaws did in fact exist on our as-received fibers and that our fibers are subject to strength degradation in their presence. And finally, as another example of the flaw sensitivity of carbon fibers, Ogihara et al. directly measured their fracture toughness and not surprisingly, found it to be quite low.[35] By notching individual fibers with focused ion beams and then tensile testing them, they determined that the fracture toughness was only 1.0–1.6 $MPa\sqrt{m}$, implying that they are very flaw sensitive indeed.

Another indication that flaw mitigation could still be partly responsible for our strength improvements is

that some other researchers have reported smoothing of existing carbon fiber surface flaws with HNO_3 treatment. Although the response to HNO_3 treatment depends on the microstructural nature of the fibers and some authors have contrarily found that HNO_3 treatment leads to increased roughness,[10,15] the works of Donnet et al., Jain et al. and Pittman et al. demonstrated the potential smoothing effect of HNO_3 treatment. After boiling high-strength carbon fibers in HNO_3 for 24 h, Donnet et al. observed significant smoothing of the surface irregularities that they had initially identified on untreated fibers. They also noted that the fiber-specific surface area (surface area per unit mass) had decreased, which they believed to be an indication of flaw removal.[11] Similarly, Jain et al. also noticed fiber surface smoothing after 15 min of refluxing concentrated HNO_3 treatment, which they believed led to fiber strength increases of 30%.[15] And like the observations reported herein, Pittman et al. observed smooth fiber surfaces with SEM analysis at all stages of HNO_3 treatment.[36]

Finally, it should also be pointed out that it is important to simply consider the diameter reductions when measuring and calculating the strength of treated fibers. Assuming that the fiber diameter does not change after extended HNO_3 treatments will lead to conclusions of lower-than-actual strength. Although several researchers have measured the strengths of fibers after various surface treatments, very little reference to the effect of diameter changes on tensile strength determinations was found in the literature. The only references found regarding bulk material loss came from Donnet et al. and Jain et al., who both noted that their high-strength fibers lost up to 32% of their weight during extended HNO_3 treatments.[11,15] They did not specifically report any diameter changes, but the weight loss suggests material removal. Other researchers have reported strength losses with HNO_3 treatments, but they did not indicate whether they considered diameter changes when calculating strengths. It is common to use the average diameter of the untreated fibers for all strength calculations, assuming that the diameter change is negligible after treatment. For example, while Jain et al. initially observed a strength increase (30%) at their shortest treatment time (15 min), all of their subsequent treatment times led to strength reductions.[15] Furthermore, both Nohara et al.[10] and Donnet et al.[11] reported fiber strength losses only, without ever observing any increases. It was shown herein that diameter change is significant with HNO_3 treatment and should be considered for post-treatment strength calculations. If Jain et al., Nohara et al. and Donnet et al. used the typical diameter of the untreated fibers for all of their strength calculations, which is commonly done, diameter reduction may help to explain the weakening they observed with treatment. By factoring the diameter reductions into their strength calculations, they may have seen less weakening or even strength stabilization, like that observed herein.

The strengths of the fibers investigated herein were found to increase through the first stage of treatment and then stabilize. The strengthening and more importantly, the stabilization of fiber strength, suggests modification of the outer layer. This most likely is a combination of the mitigation of small surface defects, along with the removal of the outer sheath layer, which has different material properties than the core. Our hypothesis is that once the organized outer layer has gradually been removed and the surface flaws minimized, the physical properties of the fiber remain largely unchanged through extended treatment times, except for diameter reduction as the less-organized graphitic structure of the core is exposed to acid attack.

(ii) Influence of HNO_3 treatment on surface chemistry and surface energy

Significant increases in carbonyl and carboxylic acid concentrations were seen during the first stage of treatment, as well as an increase in the polar surface energy. As carbonyl and carboxylic acid groups are both polar, increases in polar surface energy are expected. On the other hand, dispersive energy was found to decrease with treatment time, which can also be explained by the increase in surface oxidation. Dispersive surface energy depends on how easily the atoms or molecules are polarized and increased oxidation leads to more electronegative oxygen atoms that are known to have lower polarizability.[37] However, while the overall surface energy increases observed for relatively short HNO_3 treatment times can be attributed to surface chemistry concentration changes, later increases cannot; after approximately 40 min, the chemical concentrations of the carbon fiber surface stabilized, but the total surface energy continued to increase.

To understand this phenomenon, it is important to refer to the work of Pittman et al., who observed similar behavior.[36] Using angle-resolved XPS (ARXPS), they found that the O/C ratio on HNO_3-treated carbon fibers initially increased and then stabilized, much like that seen herein. However, when applying wet chemistry methods (NaOH uptake) to determine the total quantity of acidic functions on the fiber surfaces, they found a continuous increase without stabilization for prolonged treatments (90 min). They attributed these differences to increasing surface area caused by the formation of very small pores and crevasses on the fiber surface. These micropores, they

argued, did little to change the O/C ratio once it stabilized, but did increase the available surface area so that more functional groups could form and be available for NaOH uptake. Thus, the overall *quantity* of functional groups increased, while the surface *density* and, therefore, surface O/C ratio stayed the same. They continued their experiments by measuring surface area changes. Using adsorption of a dye of known molecular size (Methylene Blue) as well as BET adsorption, they did indeed conclude that the surface area increased with treatment time. Therefore, the behavior we observed (stabilizing O/C ratio and continuously increasing polar surface energy) could also be attributed to micropore formation. As more surface area becomes available, and the functional group quantity increases, the polar surface energy also increases, despite the fact that the density (O/C ratio) of oxidized groups remains the same.

The existence of surface pores and subsurface voids has been suggested by others as well. For example, Donnet et al.,[38] Bobka et al.[39] and Pallozzi[40] all discussed their existence, indicating that they believed them to be dependent on how the fibers are heat-treated. Specifically, fibers treated at lower temperatures (high strength fibers) are believed to have less-organized microstructures and higher levels of micropores and voids.[38] This is in accordance with Diefendorf and Tokarsky, as well as Jain et al., who also argued that high-strength fibers, which are less heat-treated, have less overall organization in their microstructures than high-modulus fibers.[15,16] Furthermore, as has already been pointed out, Diefendorf and Tokarsky also showed that carbon fiber microstructure varies across the section, with interiors having a less-organized structure than the outer sheath. Therefore, it makes sense that they would contain more voids nearer to their centers and the removal of the sheath and subsequent HNO_3 erosion would lead to the gradual exposure of more voids.

Another factor to consider when evaluating surface energy is the impact of surface pores on the circumference of the carbon fibers. Equation (1), which is used to calculate the contact angles between the test liquids and fibers, makes use of the fiber circumference. Typically, this circumference is determined by directly measuring fiber diameter with SEM, laser scan microscopy or some other method, assuming that the fiber is a smooth cylinder, and then calculating it. However, fibers with surface porosity may actually have slightly larger perimeters than their diameters would indicate and this, in turn, may affect the calculated contact angle and surface energy, to some degree. Specifically, consideration of the additional circumference from surface pores would lead to the calculation of slightly higher contact angles and lower surface energies.

The opening of surface pores with treatment may at first seem to be in conflict with the idea that acid treatment removes surface flaws and consequently improves fiber strength. The pores coming to the surface may be considered to be flaws. However, micropores and voids are likely to be very different from surface flaws that result from physical damage and abrasion. It is well known in engineering that irregular flaws with sharp edges, such as those sustained from surface damage, are much more detrimental to material strength than those with smooth or rounded edges. It is possible that opening small, rounded pores could provide additional surface area to graft more functional groups, while having minimal impact on fiber strength. These micropores may either be below a critical flaw size or sufficiently round and uniform so that they are not the dominant factor in strength, with failure first occurring due to other causes, such as other, more significant, material imperfections or inclusions. Furthermore, if these pores result from the surface exposure of internal voids and inclusions that already existed within the fiber, only moderate strength changes would be expected from their exposure to the surface. Again, it is believed that most of the strength gains result from the removal of irregular surface flaws and the differently-organized sheath material, not from just exposing internal pores to the surface.

It is not likely a coincidence that fiber diameter begins its drastic decline at the same time as the surface oxygen concentration reaches a plateau (Figure 13). It appears that the initial stages of fiber treatment are dominated by the formation of surface functional groups and when the oxidation concentration reaches a maximum, more significant material removal ensues due to chemical etching of the well-organized fiber sheath layer. At this point, more significant fiber diameter reduction begins, and this reduction is likely accompanied by the process of continuously opening micropores in the less-organized fiber core material.

Another interesting point in support of microstructural change from the sheath to the core is that the rate of material removal does not occur as one might expect. For a cylindrical shape, it would be expected that the rate of material volume loss would decrease along with the diameter (due to decreasing surface area), but the rate of diameter reduction itself would be constant. However, the rate of diameter reduction was observed to increase with HNO_3 treatment time. It would appear that as material removal progresses toward the center of the fiber and the degree of graphitic organization declines, the rate of acid attack increases. Furthermore, the exposure of less-organized interior microstructure may present increased amounts of micropores, providing even greater surface area for acid attack.

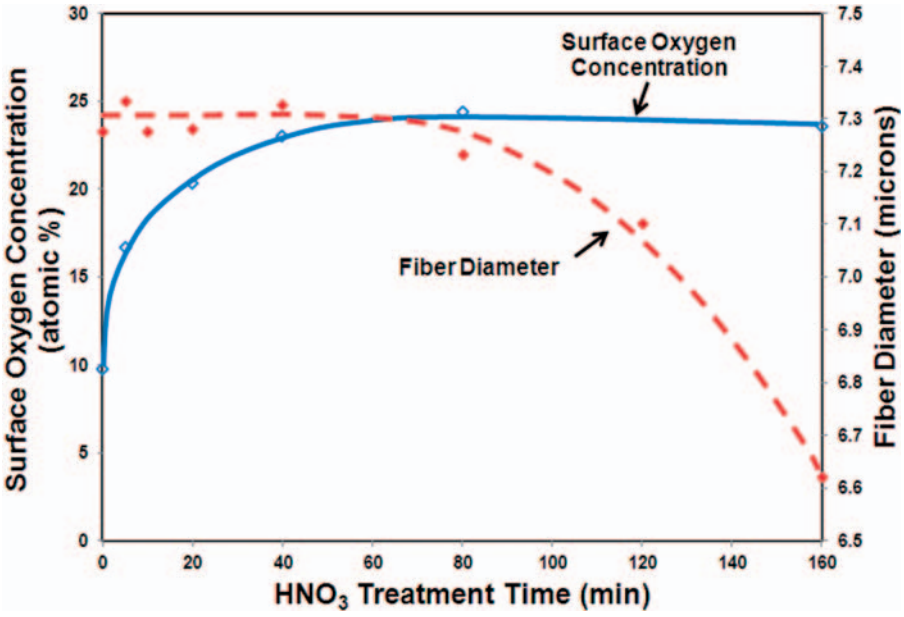

Figure 13. Comparison of the changes in surface composition (right y-axis) and diameter (left y-axis) of AS4 (unsized) fibers as a function of HNO_3 treatment time.

Conclusions

This study evaluated several properties of high-strength carbon fibers as a function of exposure time to HNO_3, including surface morphology, surface chemistry, surface energy, fiber diameter and tensile strength. It was observed that property changes occurred in two distinct stages. The first stage was characterized by increasing fiber strength and surface oxidation, which primarily consisting of carbonyl and carboxylic acid groups. During the second stage, both the fiber strength and surface chemistry stabilized, but the fiber diameter began to drastically decline in an accelerating manner. No significant concentrations of surface defects were observed via SEM at any stage, including on the as-received fibers. The only property that changed but did not appear to do so in two separate stages was the surface energy. The polar component steadily increased while the dispersive component decreased throughout the entire treatment time. The total surface energy was driven primarily by the polar energy and therefore also consistently increased.

It is believed that all of the properties evaluated are strongly dependent on the microstructure of the fibers. Specifically, high-strength carbon fibers are known to have different degrees of microstructural organization in the core material versus the outer layer, or sheath, which is better organized and aligned along the fiber axial direction. This material variation across the fiber section leads to reduced tensile strength through the creation of residual stresses within the fiber and non-uniform stress profiles under load. Therefore, removing it leads to improved fiber strength. Additionally, removal of the outer layer may also eliminate any strength-degrading surface flaws.

Acid degradation of the fiber is exceedingly slower during the first stage of treatment than in the second, which may have a couple different explanations. First, because the outer material layer has better microstructural organization, it is likely more resistant to acid attack. The second explanation stems from the fact that major diameter reduction did not begin until surface oxidation levels neared their maximums. It appears that chemical modification takes precedence over material removal in the first stage, and when that completes, more significant material loss ensues.

In the second stage of treatment, after the strength and surface chemistry stabilized, the diameter reduction accelerated towards the fiber center as less-organized material was increasingly exposed. The less organized interior material aids diameter reduction because it is more vulnerable to acid attack, but it also likely has an effect on the surface energy. Once the surface oxidation stabilized in the first stage, the surface energy would also be expected to stabilize, but it did not. Instead, it continued to steadily increase. This may be explained by the exposure of micropores contained within the increasingly disorganized graphitic structure in the core of the fiber. Without changing the overall surface functional group density (O/C ratio), they add surface area to support increasing surface energy. And because the micropores are associated with disorganized graphitic structure, more become available as the diameter is reduced to expose the less-organized core.

From a practical viewpoint, the importance of fiber property changes lies in how they will affect composite properties. For example, fiber/matrix adhesion is of great importance to composites because it allows the matrix to transfer loading to the stronger fibers. Although they possess excellent mechanical properties, untreated carbon fibers lack the ability to sufficiently chemically bond to the matrix or to coupling agents, leaving their potential mostly unrealized. However, HNO_3 treatment drastically increases carbonyl and carboxylic acid surface concentrations, making chemical bonding a much more likely possibility. Indeed, the identification of the concentration and distribution of functional groups introduced by HNO_3 treatment will help to improve composite engineering, as fiber surface bonding can be better predicted and understood. Fiber wettability (surface energy) is also important from a composites perspective because incomplete wetting leads to composite voids that create stress concentrations and prevent complete fiber/matrix bonding. Total surface energy increased with HNO_3 treatment, suggesting that fiber wettability should improve. However, caution should be exercised because these tests only evaluate the wettability of single fibers. Other factors may play a role when moving to multiple-fiber composites, such as fiber/fiber interactions. Highly reactive and energetic fiber surfaces will likely cause interactions between fibers, as well as between the fiber and matrix, which may draw the fibers together and make wetting by high-viscosity resin more difficult.[41] High tensile strength is one of the most appealing properties that carbon fibers exhibit and it was shown herein that it may be further improved through HNO_3 treatment. The combination of good wetting, strong interfacial bonding and improved fiber strength translates into the possibility of stronger, more durable carbon fiber composites.

Acknowledgements

The authors express sincere thanks to Professor D Howard Fairbrother and Kevin A Wepasnick of Johns Hopkins University for the performance of the XPS and chemical derivatization analysis, as well as the helpful comments and discussions towards the development of this document. The authors also thank Ed Drown, Mike Rich and Professor Lawrence Drzal of Michigan State University for the use of their dynamic contact angle analyzer and laser scan micrometer.

Conflict of Interest

None declared.

Funding

This work was funded by the Office of Naval Research (grant no. N00014-05-1-0341).

References

1. Drzal LT, Rich MJ and Lloyd PF. Adhesion of graphite fibers to epoxy matrices: I. the role of fiber surface treatment. *J Adhesion* 1982; 16: 1–30.
2. Fitzer E, Geigl KH and Manocha LM. Surface chemistry of carbon fibers and its influence on mechanical properties of phenolic based composites. In: *5th Industrial Conference on Carbon and Graphite*, Soc of Chem Ind, London, 1978, pp.405.
3. Lanhong X, Mase T and Drzal LT. Improving adhesion between carbon fibers and vinyl ester resins. In: *3rd Annual SPE Automotive Composites Conf*, Society of Plastics Engineers, MSU Management Education Center, Automotive & Composites Divisions, Troy, Michigan, 9–10 September 2003, pp.1–11.
4. Xu L and Drzal LT. Influence of interphase chemistry and properties on the adhesion between vinyl ester resin and carbon fibers. In *Adhesion Society 23rd Annual Technical Meeting*, Myrtle Beach, South Carolina, 20–23 February 2000, pp.1573–1582.
5. Rich MJ, Corbin SM and Drzal LT. Adhesion of carbon fibers to vinyl ester matrices. SME Technical Paper AD00-241, Society of Manufacturing Engineers, Dearborn, MI, 2000, pp.1–10.
6. Novak RC. Fracture in graphite filament reinforced epoxy. In: *Composite Materials: Testing and Design*, ASTM STP 460, Philadelphia, PA, 1969, pp.540–549.
7. McKee DW. The copper-catalyzed oxidation of graphite. *Carbon* 1970; 8: 131–139.
8. Plueddemann EP. Interfaces in polymer matrix composites. In: Broutman LJ and Krock RH (eds) *Composite Materials*, Vol. 6. New York: Academic Press, 1974, pp.217–284.
9. Donnet JB and Ehrburger P. Carbon fiber in polymer reinforcement. *Carbon* 1977; 15: 143–152.
10. Nohara LB, Filho GP, Nohara EL, et al. Evaluation of carbon fiber surface treated by chemical and cold plasma processes. *Mater Res* 2005; 8(3): 281–286.
11. Donnet JB, Dong S, Guilman G, et al. Carbon fibers electrochemical and plasma surface treatment. In: *ICCI-II, Interfaces in Polymer, Ceramic and Metal Matrix Composites*. New York: Elsevier Sci., 1988, pp.35–42.
12. Yuan LY, Shyu SS and Lai JY. Plasma surface treatments on carbon fibers, II. Mechanical properties and interfacial shear strength. *J Appl Polym Sci* 1991; 42: 2525–2534.
13. Bascom WD and Chen WJ. Effect of plasma treatment on the adhesion of carbon fibers to thermoplastic polymers. *J Adhesion* 1991; 34: 99–119.
14. Garbassi F and Occhiello E. Surface plasma treatment. *Handbook of composites reinforcements*. New York: VCH Publications, 1993, pp.625–630.
15. Jain RK, Manocha LM and Bahl OP. Surface treatment of carbon fibers with nitric acid and its influence on the mechanical behaviour of composites made with phenolic and furan as matrices. *Indian J Technol* 1991; 29: 163–172.
16. Diefendorf RJ and Tokarsky EW. The relationships of structure to properties in graphite fibers, Part I. Rensselaer Polytechnic Institute, Air Force Materials

Laboratory, Technical Report APRIL-TR-72-133, Part I, 1971.
17. Jang BZ. Control of interfacial adhesion in continuous carbon and Kevlar fiber reinforced polymer composites. *Compos Sci Technol* 1992; 44: 333–349.
18. Chang TC. Plasma surface treatment in composites manufacturing. *J Industr Technol* 1999; 15(1): 2–7.
19. Kaelble DH, Dynes PJ and Cirlin EH. Interfacial bonding and environmental stability of polymer matrix composites. *J Adhesion* 1974; 6(6): 23–48.
20. Moulder JF, Stickle WF, Sobol PE, et al. *Handbook of X-ray photoelectron spectroscopy: A reference book of standard spectra for identification and interpretation of XPS data*. Eden Prairie MN: Perkin-Elmer, 1995.
21. Langley L, Villanueva D and Fairbrother D. Quantification of surface oxides on carbonaceous materials. *Chem Mat* 2006; 18(1): 169–178.
22. Neumann AW and Tanner W. Continuous measurement of the time dependence of contact angles between individual fibres and surfactant solutions. In: *Fifth International Congress of Surface Activity B*, vol. 2, Barcelona, Spain, 1968, pp.727–734, London: Butterworths Scientific Publications.
23. Mozzo G and Chabord R. Contribution to the study of glass-resin adhesion. In: *23rd Annual Technical Conf. on Reinforced Plastics/Composites Division*, Soc. Plastics Industry, Section 9-C, 1968, pp.1–8.
24. Chen M, Yang T and Ma Z. Investigation of RF styrene plasma by emission spectroscopy. *IEEE Trans Plasma Sci* 1995; 23(2): 151–155.
25. Akhter MS, Chughtai AR and Smith DM. Spectroscopic studies of oxidized soots. *Appl Spec* 1991; 45(4): 653–665.
26. Smith DM and Chughtai AR. The surface-structure and reactivity of black carbon. *Colloids Surf A Physicochem Eng Aspects* 1995; 105(1): 47–77.
27. Boehm HP. Surface oxides on carbon and their analysis: a critical assessment. *Carbon* 2002; 40(2): 145–149.
28. Jiang ZX, Liu Y, Sun XP, et al. Activated carbons chemically modified by concentrated H_2SO_4 for the adsorption of the pollutants from wastewater and the dibenzothiophene from fuel oils. *Langmiur* 2003; 19(3): 731–736.
29. Sellitti C, Koenig JL and Ishida H. Surface characterization of graphitized carbon fibers by attenuated total reflection fourier transform infrared spectroscopy. *Carbon* 1990; 28(1): 221–228.
30. Domingo-Garcia M, Garzon FJL and Perez-Mendoza MJ. On the characterization of chemical surface groups of carbon materials. *Colloid Interface Sci* 2002; 248(1): 116–122.
31. Daniel IM and Ishai O. *Engineering mechanics of composite materials*, 2nd edn. New York: Oxford University Press, 2006, p.49.
32. Elices M and Llorca J. *Fiber fracture*. Oxford, UK: Elsevier Science Ltd, 2002, pp.9–13.
33. Griffith AA. The phenomenon of rupture and flow in solids. In: *Philos Trans R Soc.*, Series A, vol. 221, London, 1921, pp.163–198.
34. Pickering KL and Murray TL. Weak link scaling analysis of high-strength carbon fibre. *Composites: Part A* 1999; 30: 1017–1021.
35. Ogihara S, Imafuku Y, Yamamoto R, et al. Application of FIB technique to introduction of a notch into a carbon fiber for direct measurement of fracture toughness. In: *Third international symposium on atomic technology*, Journal of Physics: Conference Series, Tokyo, Japan, 191: 012009, 2009, pp.1–6.
36. Pittman CU Jr, He G-R, Wu B, et al. Chemical modification of carbon fiber surfaces by nitric acid oxidation followed by reaction with tetraethylenepentamine. *Carbon* 1997; 35(3): 317–331.
37. Anslyn EV and Dougherty DA. Introduction to structure and models of bonding. In: Murdzek J (ed.) *Modern physical organic chemistry*. Sausalito, CA: University Science Books, 2006, p.25.
38. Donnet JB and Bansal RC. *Carbon fibers*. New York: Marcel Dekker, 1984, p.232.
39. Bobka RJ and Lowell LP. Integrated research on carbon fiber composite materials. Technical Report AFML-TR-66-310, Part 1, Air Force Materials Laboratory, October 1960: 145–152.
40. Pallozzi AA. Carbon fiber reinforcement of epoxy resins. *Soc Plast Eng J* 1966; 8: 21–22.
41. Langston TA. Wettability of nitric acid oxidized carbon fibers. *J Reinf Plastics Compos* 2010; 29(14): 2156–2169.